Grafting in peri-implant bone defects by in-situ polymer deposition using a 3D pen –

in vitro/ ex vivo study

Enxertia em defeitos ósseos periimplantares por deposição polimérica in-situ através caneta 3D –

estudo *in vitro/ ex vivo*

Injerto en defectos óseos periimplantares mediante deposición de polímero in-situ a través de un

lápiz 3D – *estudio in vitro/ ex vivo*

Alícia Fabro Moraes
ORCID: https://orcid.org/0000-0002-8400-0475
Rio Grande University, Brazil
E-mail: aliciamoraes1102@outlook.com
Ândrea Leite Da Silva Lourençone
ORCID: https://orcid.org/0000-0002-3409-8347
Rio Grande University, Brazil
E-mail: andrealeitedasilvalourencone@hotmail.com
Vivyan Cordeiro Goulart
ORCID: https://orcid.org/0000-0002-9745-3131
Rio Grande University, Brazil
E-mail: vivyancordeirogoulart262@gmail.com
Ellen Dos Santos
ORCID: https://orcid.org/0000-0002-3319-4994
Rio Grande University, Brazil
E-mail:ellensantoscontatos@gmail.com
Walas Cazassa Vieira
ORCID: https://orcid.org/0000-0003-2538-4437
Rio Grande University, Brazil
E-mail:walascazassa5@gmail.com
Marcelo Ferreira Da Silva
ORCID: https://orcid.org/0000-0002-3053-3970
Rio Grande University, Brazil
E-mail: mdsodonto@yahoo.com.br
Fabiano Luiz Heggendorn
ORCID: https://orcid.org/0000-0002-2687-0165
Rio Grande University, Brazil
E-mail: fabianohegg@gmail.com

Abstract
Guided Bone Regeneration (GBR) aims to gain or maintain bone volume due to the use of barrier membranes that act for this purpose. This research aims at grafting polymeric filaments into preformed peri-implant bone defects in porcine condyles in vitro/ex vivo, stabilized and grafted with poly(lactic acid) (PLA) and poly(vinyl alcohol) (PVA) polymeric filaments, printed in-situ with a 3D printing pen. Nine porcine condyles received bone defects of 8 mm diameter and 7 mm depth, where occurred the installation of conical implants of 3.5x10 mm. After forming the bone gap region, above the apical bone anchorage, we divided the Poof Bodies (PB) according to the polymeric fill used: G.Control – without filling in the bone gap; G.PLA – with PLA scaffolds and G.PVA – with PVA scaffolds. In another step, the PVA and PLA 3D membranes were compared with the dense polytetrafluoroethylene membrane (PTFE-d). Subsequently, the SkyScan 1172 microtomograph (Bruker-µCT, Kontich, Belgium) analyzed the PB. The analysis corresponding to the total porosity revealed no statistical difference between G.Control (70.44%), G.PLA (59.99%), and G.PVA (57.66%). The closed porosity showed a statistical difference between G.Control (75.509%) and G.PVA (189.19%) and between G.PVA and G.PLA (79,093%). This study demonstrated the possibility of the polymeric filaments of PVA and PLA to fill the bone defects created, revealing an intimate contact on the surface of the implants used. The data suggested a higher porosity of the PVA filament when applied to bone defects or membrane shape.
Keywords: Bioprinting; Biopolymers; Printing, three-dimensional; Polymers.

Resumo

A Regeneração Óssea Guiada (ROG) objetiva o ganho ou a manutenção do volume ósseo, graças ao uso de membranas de barreira que atuam para tal finalidade. Esta pesquisa visa a enxertia de filamentos poliméricos em defeitos ósseos periimplantares pré-formados em côndilos suínos *in vitro/ex vivo*, estabilizados e enxertados com filamentos poliméricos poli(ácido lático) (PLA) e poli(álcool vinílico) (PVA), impressos *in-situ* com caneta de impressão 3D. Foram criados defeitos ósseos de 8 mm de diâmetro e 7 mm de profundidade em 9 côndilos suínos e instalados implantes cônicos de 3.5x10 mm. Após a formação da região de *gap* ósseo, acima da ancoragem óssea apical, os Corpos de prova (Cp) foram divididos conforme o preenchimento polimérico utilizado: G.Control – sem preenchimento no *gap* ósseo; G.PLA – arcabouço de PLA e G.PVA – arcabouço de PVA. Em outra etapa, foram comparadas as membranas de PVA e PLA 3D com a membrana de politetrafluoretileno denso (PTFE-d). Posteriormente os Cps foram analisados no microtomógrafo SkyScan 1172 (Bruker-µCT, Kontich, Bélgica). A análise correspondente à porosidade total não revelou diferença estatística entre G.Control (70,44%), G.PLA (59,99%) e G.PVA (57,66%). Já a porosidade fechada revelou diferença estatística entre G.Control (75.509%) e G.PVA (189,199%) e entre G.PVA e G.PLA (79.093%). Este estudo demostrou a possibilidade dos filamentos poliméricos de PVA e PLA preencherem os defeitos ósseos criados, revelando um contato íntimo sobre a superfície dos implantes utilizados. Os dados sugeriram uma maior porosidade do filamento de PVA quando aplicado em defeitos ósseos ou na forma de membrana.

Palavras-chave: Bioimpressão; Biopolímeros; Impressão tridimensional; Polímeros.

Resumen

El objetivo de la Regeneración Ósea Guiada (ROG) es ganar o mantener el volumen óseo, gracias al uso de membranas de barreras que actúan para tal finalidad. Esta investigación tiene como objetivo el injerto de filamentos de polímeros en defectos óseos periimplantares preformados en cóndilos porcinos in vitro/ex vivo, estabilizados e injertados con filamentos poliméricos poli (ácido láctico) (PLA) y poli (alcohol vinílico) (PVA), impresos in situ con lápiz de impression 3D. Se crearon defectos óseos de 8 mm de diámetro y 7 mm de profundidad en 9 cóndilos porcinos e instalados implantes cónicos de 3.5x10 mm. Después de la formación de la región de gap óseo, encima del anclaje apical óseo, se dividieron los cuerpos de prueba (Cp) de acuerdo al relleno polimérico utilizado: G. Control - sin relleno en el gap óseo; G. PLA – con estructura de PLA y G.PVA – con estructura de PVA. En otra etapa, fueron comparadas las membranas de PVA y PLA 3D con la membrana de politetrafluoretileno denso (PTFE-d). Posteriormente los Cps fueron analizados en el microtomógrafo (Bruker-µCT, Kontich, Belgium). El análisis correspondiente a la porosidad total no reveló diferencia estadísticamente significativa entre G control (70.44%), G.PLA (59.99%), y G.PVA (57.66%). La porosidad cerrada reveló diferencia estadísticamente significativa entre G control (75.509%) y G.PVA (189.19%) y entre G.PVA y G.PLA (79,093%). Este estudio demostró una posibilidad de rellenar los defectos óseos creados mediante filamentos poliméricos de PVA y PLA, revelando un contacto íntimo en la superficie de los implantes usados. Los datos sugieren una alta porosidad de los filamentos de PVA cuando son aplicados en defectos óseos o en la forma de membrana.

Palabras clave: Bioimpresión; Biopolímeros; Impresión tridimensional; Polímeros.

1. Introduction

Among the different matrix manufacturing techniques, bioprinting applied directly to an injured site during surgery stands out, called intraoperative bioprinting or in-situ or in-vivo bioprinting, allowing the reconstruction of different craniomaxillofacial features such as bones, skin, and composite tissues, in an associated or isolated way (Moncal et al., 2021). This developing process allows bone remodeling through the association of osteoprogenitor cells during cell proliferation, differentiation, and matrix formation (Wang, et al., 2020).

The use of manual printers and 3D pens has been popularized in recent years due to their low cost and practicality. Thus, many materials are widely studied, such as thermoplastic filaments of acrylonitrile butadiene styrene, polylactic acid (PLA), polyvinyl alcohol (PVA), polyethylene terephthalate glycol, polycarbonate, and nylon (Santana, et al., 2018).

Porous polyethylene does not reabsorb nor degrades and has the advantage of allowing internal vascular and soft tissue growth after one week and internal bone growth after three weeks. The porous polyethylene is characterized as non-antigenic, anti-allergic, non-absorbable, highly stable, easily fixated, and available in various formats for reconstruction (Maia, et al., 2010).

PLA is a linear aliphatic synthetic polymer that exhibits biodegradability, biological absorption, biocompatibility, mechanical tensile strength, modulus of elasticity, thermal stability, and low environmental impact. In addition, its melting point is 180 °C (Santana et al., 2018).

PVA is a biodegradable, water-soluble, non-toxic, hydrophilic synthetic polymer produced through the hydrolysis of vinyl acetate (Prasadh, et al., 2018; Basa et al., 2021), widely used in topical pharmaceutical, ophthalmic formulations and drug-loaded pharmaceutical microsponges. In solid pharmaceutical formulations, PVA can be used as tablet coating. This polymer is also the most widespread support in 3D printing (Basa et al., 2021).

Bone defects undoubtedly tend to be a challenge for several areas of dentistry, particularly in oral and maxillofacial surgery, periodontics, and implantology. Repair of these bone defects is challenging even when the correct Guided Bone Regeneration (GBR) technique is applied (Prado et al., 2006; Araujo, et al., 2022).

In parallel, osseointegration is the direct anchoring of a dental implant through the formation of bone tissue around the implant without the growth or development of fibrous tissue at the bone-implant interface, which ensures its stability (Mantovani Junior, 2006; Araujo et al., 2022). In this context, the different bone defects are challenging in the fixation of implants and may face partial or total fenestrations of the vestibular wall, leading to exposure of the threads of this implant after its installation (Consolaro, et al., 2010).

As biomaterials are developed, certain defects can be corrected, leading to bone volume gain. The properties of these biomaterials range from osteogenic to osteoinductive, releasing bone morphogenic proteins and allowing undifferentiated mesenchymal cells to differentiate into osteoblasts and chondroblasts, initiating the bone remodeling process (Okamoto, et al., 1973).

Thus, this study aims to analyze the grafting of polymeric filaments in peri-implant bone defects performed in porcine condyles in vitro/ex vivo, stabilized and grafted with PLA and PVA polymeric filaments, printed in-situ with a 3D printing pen.

2. Methodology

This study was submitted to the ethics committee on animal use of the Grande Rio University under the number 045/2021.

This research was based on the quali-quanti method. Qualitative analyzes were based on the information and details provided through the 3D scanning images. Quantitative analyzes were based on reconstruction software and analysis of 3D tomographic images. Thus, the analyzes were completed facilitating the understanding of the results obtained (Pereira, et al., 2018).

In this qualitative-quantitative in vitro and ex-vivo research we used five dissected porcine mandibles had the condyle region sectioned with carborundum discs. Then, nine condyles received bone defects using a trephine drill with 8 mm diameter and 7 mm depth, at an angle of 90° in relation to the bone surface and at 500 RPM with a Driller motor (BLM350 - Driller). We store the specimens at –2° C, remaining at room temperature until reaching 23° C during the tests.

Subsequently, we installed one conical implant of 3.5x10 mm (Singular, Parnamirim, RN) in each condyle, totaling nine PB, following the milling sequence with lance drills and 2.0 and 3.5 twist drills. Located in the central region of the defects, the implants had an apical intraosseous anchorage of 4 mm and a final installation torque from 10 to 20 N at 500 RPM. After forming the bone gap region above the apical bone anchorage, the proof bodies (PB) were divided according to the polymeric filling used: group G.Control with no filling in the bone gap; Group G.PLA with PLA scaffolds, and Group G.PVA with PVA scaffolds. A 3D pen deposited the filaments in situ. We studied the groups in triplicate for each condition (Table 1 and Figure 1).

Table 1 - Distribution of the proof bodies (PB) in relation to the scaffold used to fill the bone gap.

Proof Body	Final installation torque	Group and scaffold used
1	20N	G.Control - No filling
2	20N	
3	20N	
4	20N	G.PLA
5	15N	
6	10N	
7	10N	G.PVA
8	10N	
9	10N	

Source: Authors.

Figure 1 – Preparation of the proof bodies. Formation of the bone defect (Figure A), followed by the installation of the osseointegrated implant, with a bone gap between the implant surface and the medullary wall (Figure B). Filling of the bone gap with polymeric PLA scaffolds (Figure C) and PVA scaffolds (Figure D).
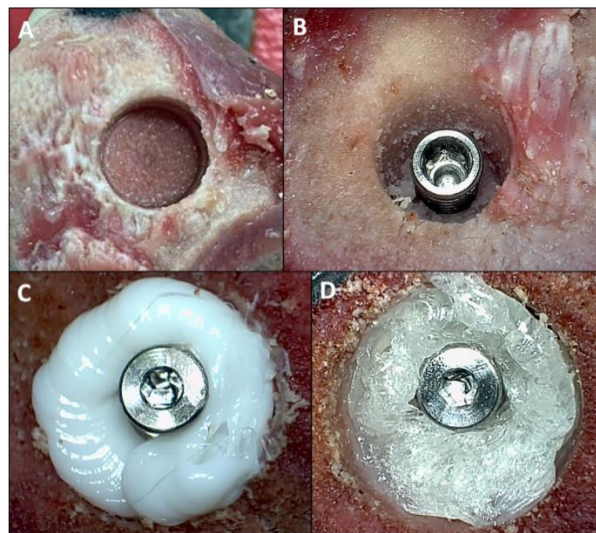
Source: Authors.

2.1 3D Pen

We used commercial filaments of PVA and PLA of 0.75 mm. A 3D pen extrudes the filaments at 200°C and at a speed of 30 mm/s (Saywe SMA-1 Plus). Filament deposition occurred directly in the bone gaps until the filling reached the cortical bone crest of the PB.

2.2 Microtomographic Analysis

A SkyScan 1172 microtomography (µCt) (Bruker-µCT, Kontich, Belgium) analyzed all PB and membranes. The µCT had the following common parameters for image acquisition in all stages: voltage of 50 Kvp, source current of 800 µA, flat-field correction, Al 0.5 filter, pixel size of 18.99 µm, exposure time of 4000 ms, rotation step of 0.5 and Frame Averaging 3.

The NRecon program (SkyScan, Kontich, Belgium) reconstructed and processed the images obtained from µCT adjusting the parameters: ring artifacts reduction in 7, Beam-hardening correction in 46%, Gaussian kernel smoothing and defect pixel masking in 50%, and misalignment compensation.

Then, the DataViewer program (SkyScan, Kontich, Belgium) analyzed the reconstructed images for visualization and 2D evaluation of the coronal, transverse, and sagittal axes, using the Hounsfield Unit to evaluate the pixel intensity of the artifacts found in the PB.

The CTan program (SkyScan, Kontich, Belgium) also analyzed the images and delimited the regions of interest, proceeding to the thresholding and binarization of the images, adjusting the histogram to evidence the suggestive artifacts of voids and bubbles. Ultimately, the CtVox software (SkyScan, Kontich, Belgium) presented the 3D images for visual evaluation.

GraphPad Prisma 5.01 software (Graph Pad Software Inc) performed the statistical analysis of the data, with analysis of variance (One-Way ANOVA) and complementary Tukey post-test, with a significance level of 5% ($p < 0.05$).

2.3 PVA and PLA Membranes

In parallel, we extruded the PVA and PLA filaments on a glass surface of 3x3 cm, in a single layer of deposition, using the same extrusion parameters applied above. These PVA and PLA membranes were developed in triplicate and analyzed on µCt.

This step involves a membrane based on dense polytetrafluoroethylene (PTFE-d), Ti-250 cytoplast membrane (Implacil De Bortoli, Osteogenics Biomedical, São Paulo, Brazil) with titanium reinforcement as a control sample. This membrane is non-resorbable and used in GBR surgeries, with porosity less than 0.3 µm, characterized by having greater resistance to bacterial penetration, protecting the bone and the implant below this membrane (Maridati, et al., 2016).

For the microtomographic analysis of the PTFE membrane, we selected a quadrant composed exclusively of PTFE, without titanium reinforcement, considering the generation of artifacts created during the scanning of the metal structure. Here, the adequated parameters due to the low radiolucids of the PTFE are 50 Kvp voltage, source current of 800 µA, flat-field correction, no filter, pixel size of 18.99 µm, exposure time of 1700, rotation step of 0.3, and Frame Averaging 3.

3. Results

From the analysis performed at µCt, information corresponding to total porosity (Po(tot)%) obtained for G.Control is an average of 7.045 Po(tot)%, corresponding to the void of the bone gap; G.PLA presented an average of 6.00 Po(tot)%, and G.PVA has an average of 5.76 Po(tot)%. Statistical analysis showed no significant difference in total porosity between the groups. Analyzing separately the open porosity (Po(op)%) and the closed porosity (Po(cl)%), no statistical difference for Po(op)% between the groups, whereas the mean values are 7.017 Po(op)% for G.Control, 5.998 Po(op)% for G.PLA, and 5.764 Po(op)% for G.PVA. On the other hand, the Po(cl)% data revealed a statistical difference between G.Control (3.729 Po(cl)%) and G.PVA (8.046 Po(cl)%) and between G.PVA and G.PLA (3.320 Po(cl)%) (Graph. 1).

The analysis of surface objects (Obj.S mm^2), applied to analyze the surface area of all solid things within the volume of interest (VOI), allowed the correlation with the surface area of the exposed implants. The values are higher in G.Control (6.024 Obj.S mm^2), while in the G.PVA (4.008 Obj.S mm^2) and G.PLA (3.457 Obj.S mm^2) groups the contact of the polymers

with the implant surface reduced this relationship of surface objects, suggesting a filling relationship of the bone gaps contacting the implant surface (Graph. 1).

Graph 1 - Analysis of total porosity, closed and open porosity, surface objects, the total volume of pore space, and volume of open pore space.
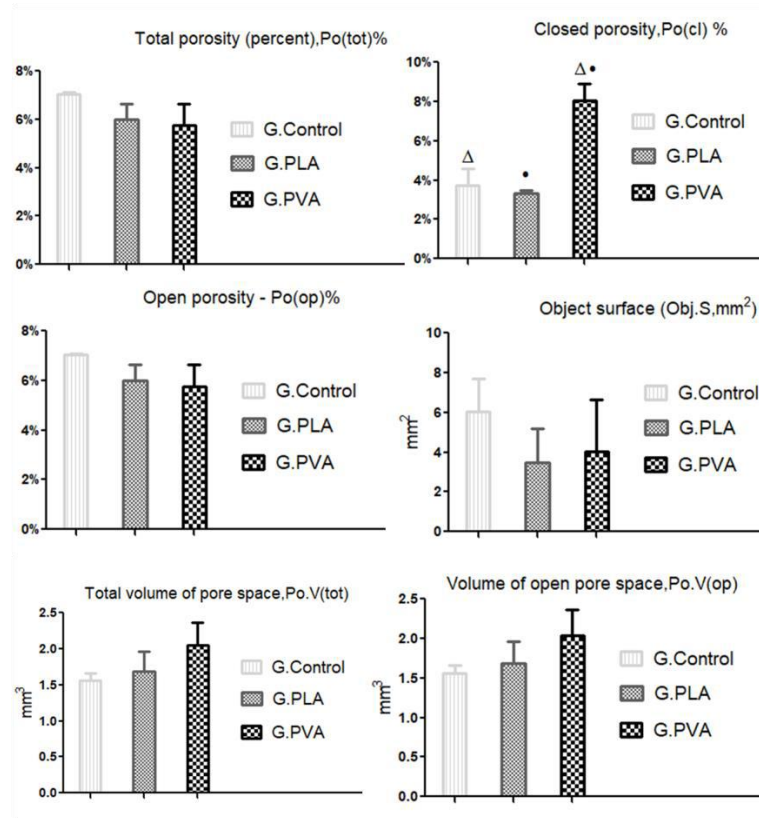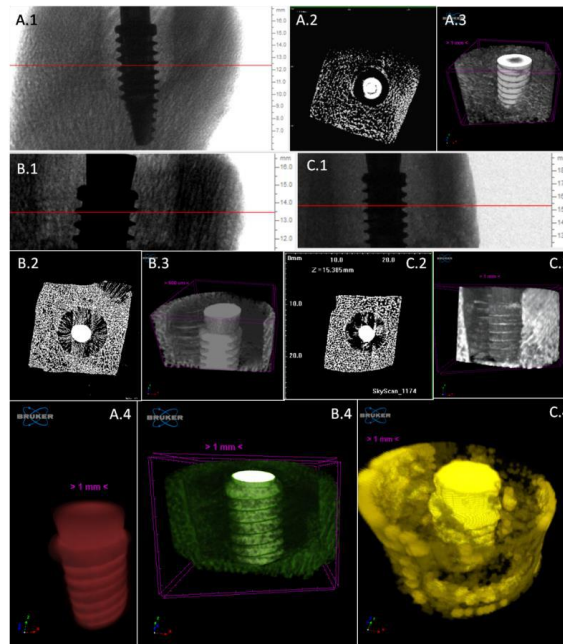

Source: Authors.

$\Delta\bullet$ = Statistical difference between samples.

The parameters of total porous space volume (Po.V(Tot)%) and open porous space volume (Po.V(op) mm^3) are correlated to the porosity of the biomaterial, corresponding to black pixels surrounded by white pixels for Po.V(Tot), or partially surrounded by white pixels for Po.V(op). These two parameters are greater for G.PVA (2.042 Po.V(Tot)% and 5.764 Po.V(op) mm^3), followed by G.PLA (1.682 Po.V(Tot)% and 5.998 Po.V(op) mm^3) and G.Control (1.561 Po.V(Tot)% and 7.017 Po.V(op) mm^3). However, the data did not present statistical differences between the groups.

Analyzing all the data, we can suggest a greater porosity in the G.PVA group associated with a greater filling of the bone gap by contacting the metallic surface of the implant.

The 3D analysis in the CTan program revealed implants anchored with bone defects in the G.Control, G.PLA, and G.PVA groups, forming the bone gaps. On the other hand, the analysis of the binarized images in the same program demonstrated the grafting performed in the G.PLA and G.PVA groups, filling the bone gaps, while the bone gaps remained present in G.Control (Figure 2).

Figure 2 - Photomicrographs of the groups 3D analysis. Implants anchored with bone defects in G.Control (Fig. A.1), G.PLA (Fig. B.1), and G.PVA (Fig. C.1), with an indication of the axial section area (red line) binarized, in the CTan program, in the G.Control (Fig. A.2), G.PLA (Fig. B.2) and G.PVA (Fig. C.2) groups, demonstrating the grafting relationship performed by the polymers in the bone gaps. The contact relationship of the polymers with the surface of the implants analyzed in the 3D images through the CtVox program demonstrates the integrated surface of the implant in the G.Control group (Fig. A.3 and A.4) and the filling of the polymers with a surface coating of the implants in G.PLA (Fig. B.3 and B.4) and G.PVA (Fig. C.3 and C.4).

Source: Authors.

The contact relationship of the polymers with the surface of the implants analyzed in the 3D reconstruction through the CtVox program complemented the analyzes, corroborating the previous findings. The 3D reconstruction demonstrated the integrated surface of the implant in the G.Control. At the same time, the coating of the surface of the implants in G.PLA and G.PVA and the bone gaps throughout the extent of the defect produced are visible (Figure 2).

The analysis detected the density difference between the polymers. In the reconstruction of G.PVA, a less dense polymer, we notice intercalated areas of porosity. In contrast, the images of G.PLA, a polymer denser than PVA, revealed areas with horizontal extensions and a better distribution of the radiodense regions (Figure 2). These data corroborated the statistical difference found for closed porosity in G.PVA and G.PLA groups.

3.1 PVA and PLA membranes

Microtomographic analysis of the membranes revealed a total porosity (Po(tot)%) and an open porosity (Po(op)%) higher in the PTFE membrane (9.167 Po(tot)% and 9.167 Po(op)%) compared to the PLA (8.102 Po(tot)% and 8.099 Po(op)%) and PVA (7.875 Po(tot)% and 7.874 Po(op)%) membranes. While the closed porosity (Po(cl)%) is lower in the PLA membrane (1.394 Po(cl)%) and PVA (4.801 Po(cl)%) compared to the PTFE membrane (6.468 Po(cl)%).

The average object surface (Obj.S mm^2) is lower in the PVA membrane (2,693 Obj.S mm^2) in relation to the PLA membrane (3,256 Obj.S mm^2), demonstrating a higher filling ratio in the PLA membrane due to the higher average, but this

data also suggests a higher porosity in the PVA membrane, justified by the lower filling of the volume in the area of interest. The PTFE membrane presented 6,468 Obj.S mm^2, explaining the higher density of this membrane compared to PLA and PVA. Corroborating this argument, the volume averages of open pore space (Po.V(op) mm^3) and the total volume of pores space (Po.V(Tot) mm^3) are lower in the PVA membrane (5.467 Po.V(op) mm^3 and 5.450 Po.V(Tot) mm^3) compared to those of the PLA membranes (5.671 Po.V(op) mm^3 and 5.672 Po.V(Tot) mm^3) and PTFE (7.874 Po.V(op) mm^3 and 7.874 Po.V(Tot) mm^3). After analyzing this set of data corroborated by the closed porosity, we can suggest a greater porosity of the PVA membrane.

The analysis of the 3D reconstructed membranes in CtVox and Ctan programs suggested the presence of numerous pores of different sizes, indicating greater intensity in the PVA membrane. As it is a manual 3D deposition, the spaces between the deposited filaments are noted. The binarized reconstructions in the Ctan also suggested a higher pore intensity in the PVA membranes than the PLA membranes (Figure 3). In contrast, PTFE membrane reconstruction did not show visible pores, suggesting a highly compact material (Figure 3).

Figure 3 - 3D reconstruction of the membranes. Binarized images in the CTan program of the PVA membrane (FigureA.1) and the PLA membrane (Figure B.1) demonstrate the presence of pores in the PVA membrane (Figure A.1, yellow arrow). 3D reconstruction on Ctvox indicating pores in the PVA membrane (Figure A.2 and A.3, yellow arrow) and on the PLA membrane (Figure B.2 and B.3, yellow arrows) and the presence of voids between the filaments (Figure A.2 and B.2, red arrows). PTFE membrane reconstructed in the CTan program (Figure C1 and C.2). The region in the square at C.1 represents the area selected as the volume of interest of the PTFE membrane, with the binarized image presented in C.2.
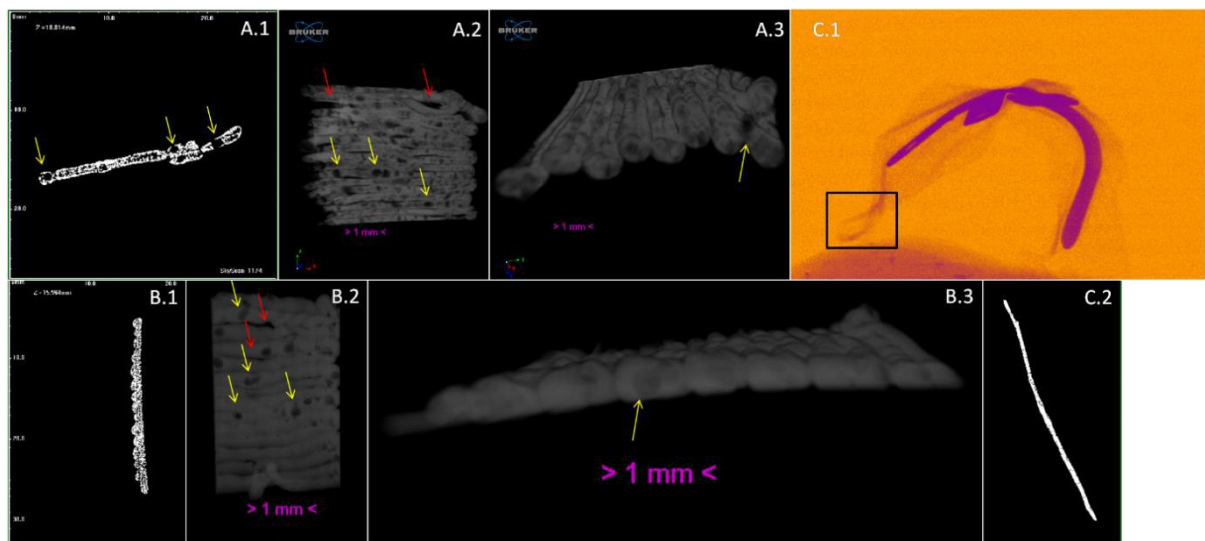
Source: Authors.

4. Discussion

This study is based on using different regenerative techniques associated with biomaterials. The main objective of this technique is to obtain the vertical and horizontal bone volume in bone edges, aiming to minimize bone remodeling after tooth extraction for the installation of integrated bone implants (Costa et al., 2021; Sanz et al., 2019).

Different biodegradable and non-biodegradable materials are investigated in the application of GBR and should present biocompatibility, semipermeability, integration into host tissues, clinical maneuverability, and space maintenance capacity (Warrer, et al., 1993).

If bone defects are not reduced, they can interfere with or even make prosthetic rehabilitation impossible. During the installation of osseointegrated implants in regions with atrophy or severe bone defects, stability can be compromised, causing premature losses, besides aesthetic and functional defects. Therefore, inadequate bone volume for implant placement is a critical clinical problem, determining the need to insert bone grafts to ensure adequate bone volume and provide greater stability, leading to a better prognosis (Herford & Dean, 2011).

The present study adopted in-situ PVA and PLA filaments in the proof of concept. Still, the data suggested the complete filling of the bone defect using a 3D pen, which may represent a future development in the GBR bone grafting technique.

Based on the microarchitecture characteristic of the scaffold, the feasibility and level of precision of the manufacturing process can be evaluated (Ho & Hutmacher, 2006). The microarchitectures of the scaffolds also influence the mechanical strength and biological functionality, and pore size, porosity, and surface area/volume ratio can be evaluated through analysis (Ho & Hutmacher, 2006). The analysis of the membranes indicated a lower porosity in the PTFE membrane, followed by the PLA and PVA, as the one with greater porosity. The data are justified once the PTFE membrane is non-absorbable, and this high porosity is unnecessary. Structurally, the membranes may present perforations to improve the conditions for bone neoformation. Rigid membranes, such as PTFE membranes, act as a substrate so isolated cells can fix and grow to form tissue (Costa et al., 2016).

Contrastingly, the PVA membrane with greater porosity indicates a possible absorption characteristic in the body. The absorbable membranes are advantageous as they do not require a second surgical time for removal, being degraded or incorporated by the body throughout the regeneration process (Rakhmatia, et al., 2013). In this context, absorbable membranes propose greater bone formation in relation to non-absorbable membranes (Costa et al., 2021).

The biological membrane materials must be physically capable of allowing adequate modeling of the graft, the implant, and the bone structure. A hardness is necessary so it does not deform after being adjusted in place nor move easily, thus preventing inflammation (Costa et al., 2016). The versatility of developing PVA or PLA membranes or scaffolds, directly at the surgical site, may encompass these different requirements in this type of biomaterial.

High porosity may represent a low tensile strength since stress causes the existing cracks to spread (De Oliveira, et al., 2007), however, porosity is desirable in scaffolds for biomaterial use in grafting procedures. The microtomographic analyses obtained information on total porosity, open porosity, closed porosity, and surface objects, identifying in the last two items desirable porosity specifications associated with the uniform distribution of polymers in PVA or PLA scaffolds, presenting better closed porosity and surface objects in the first filament.

The high porosity and surface area for volume are fundamental characteristics of uniform cellularity, enabling tissue fixation and neoformation. An ideal porosity would be 90%, allowing the diffusive transport of cells within the scaffolds (Ho & Hutmacher, 2006). Nevertheless, such a high porosity could compromise the mechanical properties of scaffolds (Ho & Hutmacher, 2006). In the presented data, the G.PVA group reached a closed porosity of approximately 90%, while the total porosity in G.PLA and G.PVA groups was close to 60%, suggesting the possibility of being biomaterials susceptible to cell neoformation.

Once the total porosity is based on the volume of all open and closed pores, of the VOI selected in each sample, the closed porosity data is divergent. However, the Po(cl)% analysis considers the total solids plus the volume of closed pores within the VOI, suggesting the filling of the greater peri-implant bone defect in the G.PVA group, followed by the G.PLA group, once this analysis allows interpreting the reduction in open porosity, filling the peri-implant bone defect as best as possible.

Some factors may affect or intervene in micro-CT porosity measurements. By increasing the segmentation threshold, more pixels of other tones are included in the segmented phase, changing the quantification of the open porosity. The presence of metallic implants led to the appearance of artifacts, removed with the increase of the segmentation threshold suggesting changes in the open porosity. This occurrence can elucidate the difference in the data found between open pores and closed pores during the analysis of the groups.

The proposed methodology detected closed and open pores in all PB. The object's surface function differentiated the analysis between open and closed pores, discarding black objects in which only the dark objects connected to the surface are visible in black.

Previously, Ho and Hutmacher (2006) reported using µCT in scaffolding research, as they characterized the morphology in poly (L-lactide-co-DL-lactide) and poly-e-caprolactone scaffolds manufactured through extrusion deposition. Nowadays, a diversity of research on PLA and PVA is ongoing (Ho & Hutmacher, 2006; Santana, et al., 2018).

Thermoplastic semi-crystalline polymers are excellent candidates for developing tissue-engineered scaffolds as they are easy to process and present adjustable properties. In parallel, synthetic polymers can be an option for scaffolds applicability in hard tissues, presenting physical characteristics such as material stiffness, roughness, and topography that are desirable for cell neoformation (Calore et al., 2021). Calore et al. (2021) indicated that in an osteogenic environment, human mesenchymal stromal cells responded more to surface roughness than to surface stiffness of different scaffolds.

The applicability of in-situ printed PLA and PVA filaments on bone defects generating the stability of osseointegrated implants has not yet been explored. Therefore, the data exposed in this study bring an innovative possibility of polymeric biomaterials in implant dentistry to minimize early loss of osseointegrated implants and its usage in the GBR technique.

5. Conclusion

This study demonstrated the possibility of using a 3D pen in situ as an instrument in GBR surgery, completely filling peri-implant bone defects with the implant already installed. In addition, the polymeric filaments of PVA and PLA demonstrated the ability to fill the bone defects created, revealing an intimate contact on the surface of the implants.

The data suggested a higher porosity of the PVA filament when applied to bone defects or membrane shape.

Once this is a proof-of-concept study, additional data are still necessary until the feasibility of applying the materials presented can be concluded.

Acknowledgments

References

Araujo, L. C., Dos Santos, Y. B. C., Leite, R. S., & Heggendorn, F. L. (2022). Extraction associated with L-PRF grafting and immediate installation - Case reports. *Research, Society and Development*, 11(3), e47211326563. doi.org/10.33448/rsd-v11i3.26563

Basa, B., Jakab, G., Kállai-Szabó, N., Borbás, B., Fülőp, V., Balogh, E., & Antal, I. (2021). Evaluation of biodegradale PVA-Based 3D Printed Carriers during Dissolution. *Materials*, 14(6), 1350. doi.org/10.3390/ma14061350

Calore, A. R., Srinivas, V., Anand, S., Abillos-sanches, A., Looijmans, S. F. S. P., Van Breemen, L. C. A., & Moroni, L. (2021). Shaping and properties of thermoplastic scaffolds in tissue regeneration: The efect of thermal history on polymer crystallization, surface characteristics and cell fate. *Journal of Materials Research*, 36(19), 3914-35.10.1557/s43578-021-00403-2

Consolaro, A., Carvalho, R. S., Francischone Jr, C. E., Consolaro, M. F. M. O., & Francishone, C. E. (2010). Saucerização de implantes osseointegrados e o planejamento de casos clínicos ortodônticos simultâneos. Dental Press J. Orthod, 15(3), 19-30. doi.org/10.1590/S2176-94512010000300003

Costa, V. C. F., Bianchi, C. M. P. C., Filho, A. C. G., Crepald, M. L. S., Oliveira, B. L. S., Aguiar, A. P., & Deps, T. D. (2021). Membranas utilizadas em regeneração óssea guiada (ROG): Características e indicações. *Revista Faipe*, 11(1), 48-57. https://www.revistafaipe.com.br/index.php/RFAIPE/article/view/230

De Oliveira, A. A. R., De Oliveira, J. E., Oréfice R. L., Mansur H. S., & Pereira M. M. (2007). Avaliação das propriedades mecânicas de espumas híbridas de vidro bioativo/álcool polivinílico para aplicação em engenharia de tecidos. Revista Matéria, 12(1), 140 – 149. doi.org/10.1590/S1517-70762007000100018

Herford, A. S., & Dean, J. S. (2011). Complications in bonegrafting. Oral Maxillo fac Surg Clin North Am., 23(3), 433-42. 10.1016/j.coms.2011.04.004.

Ho, S. T., & Hutmacher, D. W. (2006). A comparison of micro CT with other techniques used in the characterization of scaffolds. *Biomaterials,* 27(8), 1362-76. doi.org/10.1016/j.biomaterials.2005.08.035

Maia, M., Klein, E. S., Monje, T. V., & Paguosa, C. (2010). Reconstrução da estrutura facial por biomateriais: Revisão de literatura. *Rev. Bras. Cir. Plást.*, 25(3), 566-72. doi.org/10.1590/S1983-51752010000300029

Mantovani Junior, M. (2006). Análise histológica de defeitos ósseos preenchidos com biomateriais e associados a implantes osseointegrados. Estudo em cães (Dissertação de mestrado). Universidade Estadual Paulista, Faculdade de Odontologia de Araraquara, São Paulo, SP, Brasil. http://hdl.handle.net/11449/96180

Maridati, P. C., Cremonesi, S., Fontana, F., Cicciù, M., & Maiorana, C. (2016). Management of d-PTFE Membrane Exposure for Having Final Clinical Success. *Journal of Oral Implantology*, 42(3), 289-91. 10.1563/aaid-joi-D-15-00074

Moncal, K. K., Gudapati, H., Godzik, K. P., Heo, D.N., Kang, Y., Rizk, E., & Ozbolat, I. T. (2021). Intra-Operative Bioprinting of Hard, Soft, and Hard/Soft Composite Tissues for Craniomaxillo facial Reconstruction. *Atty. Funct. Specialization*, 31, 1-15. doi: 10.1002/adfm.202010858

Okamoto, T., Perri, A. C. C., & Milanezi, L. A. (1973) Implante de poliuretano em alvéolos dentais. Estudos histológicos em ratos. *Rev. Fac. Odontol. Aracatuba,* 2(1), 19-25. <http://hdl.handle.net/11449/219029>.

Pereira, A. S., Shitsuka, D. M., Parreira, F. J., & Shitsuka, R. (2018). Metodologia da pesquisa científica**.** Santa Maria, RS: UFSM. https://repositorio.ufsm.br/bitstream/handle/1/15824/Lic_Computacao_Metodologia-Pesquisa-Cientifica.pdf?sequence=1

Prado, F. A., Anbinder, A. L., Jaime, A. P., Lima, A. P., Balducci, I., & Rocha, R. F. (2006). Defeitos ósseos em tíbia de ratos: padronização do modelo experimental. *Rev. odontol. Univ. Cid. Sao Paulo*, 18(1), 7-13.

Prasadh, S., Suresh, S., & Wong, R. (2018). Osteogenic of Graphene in bone tissue engineering scaffolds. *Materials,* 11(8), 1430. doi.org/10.3390/ma11081430

Rakhmatia, Y. D., Ayukawa, Y., Furuhashi, A., & Koyano, K. (2013). Current barrier membranes: titanium mesh and other membranes for guided bone regeneration in dental applications. *J. Prosthodontic Res*., 57(1), 3-14. 10.1016/j.jpor.2012.12.001.

Santana. L., Alves, J. L., Netto, A. C. S., & Merlini, C. (2018). Estudo comparativo entre PEGT e PLA para impressão 3D através de caracterização térmica, química e mecânica. *Revista Matéria*, 23(4), e-12267. doi.org/10.1590/S1517-707620180004.0601

Sanz, M., Dahin, C., Apatzidou, D., Artzi, Z., Bozic, D., Calciolari, E., & Schliephake, H. (2019). Biomaterials and regenerative technologies used in bone regeneration in the craniomaxillofacial region.: Consensus report of group 2 of the 15th European Workshop on Periodontology on Bone Regeneration. *J Clin Periodontol*, 46(21): 82-91, 2019. 10.1111/jcpe.13123

Wang Y., Gao, M., Wang, D., Sun, L., & Webster, T. J. (2020). Nanoscale 3D Bioprinting for Osseous Tissue Manufacturing. *International Journal of Nanomedicine*, 15, 215–226.

Warrer, K., Karring, T., & Gotfredsen, K. (1993). Formação do ligamento periodontal em torno de diferentes tipos de implantes dentários de titânio. I. O sistema de implante tipo parafuso auto-roscante. *Revista de Periodontologia*, 64(1), 29-34. doi.org/10.1902/jop.1993.64.1.29